

Optimal lane-changing control at motorway bottlenecks*

Claudio Roncoli, Nikolaos Bekiaris-Liberis, and Markos Papageorgiou

Abstract—We propose an optimal feedback control strategy for lane-changing control at bottleneck locations, assuming that a percentage of vehicles, equipped with vehicle automation and communication systems, are capable of receiving and executing specific lane-changing orders or recommendations. Based on a simplified multi-lane motorway traffic flow model, we formulate an optimal feedback control problem, cast as a linear quadratic regulator problem, aiming at maximising the throughput at bottleneck locations, via optimal lane assignment of vehicles upstream of the bottleneck. The feedback control decisions are based on appropriate choice of set-points for traffic densities and real-time measurements of the state of the system. We also present an extremum seeking algorithm to seek the optimal set-points using only the measurement of a cost that is representative of the achieved traffic conditions. The proposed strategy is tested on a nonlinear first-order macroscopic multi-lane traffic flow model, which accounts also for the capacity drop phenomenon.

I. INTRODUCTION

In the near future, Vehicle Automation and Communication Systems (VACS) are expected to revolutionise the features and capabilities of individual vehicles. Among the wide range of introduced VACS, some may be exploited to interfere with the driving behaviour via recommending, supporting, or even executing appropriately designed traffic control tasks, providing unprecedented opportunities to improve traffic control performance [1]. On the other hand, the uncertainty in the future development of VACS calls for the design of control strategies that are robust with respect to the different types of these new systems, as well as to their penetration rate.

A promising feature that can be exploited for traffic management is lane-changing control. In fact, particularly at bottleneck locations (e.g., lane-drops, on-ramp merges), human drivers usually perform suboptimal lane-changes based on erroneous perceptions, which may trigger congestion, and, thus, deteriorate the overall travel time [2], [3]. In case a sufficient percentage of vehicles are equipped with VACS having vehicle-to-infrastructure (V2I) capabilities and appropriate lane-changing automatic controllers or advisory systems, the overall throughput at the bottleneck location may be improved by execution of specific lane-changing commands dictated by a central decision maker.

*The research leading to these results has received funding from the European Research Council under the European Union's Seventh Framework Programme (FP/2007-2013) / ERC Grant Agreement n. 321132, project TRAMAN21.

Claudio Roncoli, Nikolaos Bekiaris-Liberis, and Markos Papageorgiou are with the School of Production Engineering and Management, Technical University of Crete, Chania 73100 Greece {croncoli, nikos.bekiaris, markos}@dssl.tuc.gr

The problem of assigning traffic flow among lanes for motorways under fully automated or semi-automated driving has been tackled in numerous works during the last decades. In the seminal work [4], a hierarchical framework for a fully automated motorway is defined, where the decisions on the lane-changing behaviour of vehicles are addressed within the link layer, which consists of a set of parallel decentralised link controllers, each of them addressing a corresponding motorway link (of about 2 km in length). Following this framework, several strategies have been proposed to solve the problem of lane assignment within the link layer, designing control methodologies suitable for real-time applications, including [5], [6], [7], [8], [9], [10].

Recently, a combined lane-changing and variable speed limits control strategy was developed [3], with the purpose of avoiding lane changes in the immediate proximity of a bottleneck, which, especially in the case of heavy vehicles, may lead to premature triggering of congestion. In particular, lane-changing commands delivered as recommendation to the drivers, are defined according to a set of case-specific rules. Furthermore, in [11], a multi-agent decentralised framework is proposed, with the aim of performing cooperative lane-changing tasks based on information exchange between vehicles and a road side unit located at a bottleneck.

In this paper we propose an optimal feedback control strategy, formulated as a linear quadratic regulator, where the solution is applied in the form of a linear state-feedback control law, which is highly efficient in real-time, even for large-scale networks. We show that, with appropriate modelling treatments, our control strategy can be applied to any network configuration. The control strategy aims at regulating the lane assignment of vehicles upstream of a bottleneck location so as to maximise the bottleneck throughput. Since the methodology requires the knowledge of the optimal set-points, namely, the critical densities at bottleneck locations, which may not be available a priori, we also employ a non-model-based real-time optimisation technique, namely, extremum seeking [12], to identify them, with the aim of minimising a performance index, namely the total travel time over a finite time horizon.

The remaining paper is structured as follows. Section II describes the design of the proposed control framework for multi-lane motorways; Section III presents simulation experiments, based on a first-order macroscopic traffic flow model featuring the capacity drop phenomenon, in order to evaluate the effectiveness of the methodology; while the paper concludes with Section IV, where the main results are highlighted and further research challenges are proposed.

II. LANE-CHANGING-BASED OPTIMAL CONTROL OF MULTI-LANE MOTORWAYS AT BOTTLENECKS

A. Linear multi-lane traffic flow model

We consider a multi-lane motorway that is subdivided into $i = 0, \dots, N$ segments of length L_i , while each segment is composed of $j = m_i, \dots, M_i$ lanes, where m_i and M_i are the minimum and maximum indexes of lanes for segment i . We denote each element of the resulting grid (see Fig. 1) as ‘‘cell’’, which is indexed by (i, j) . The model is formulated in discrete time, considering the discrete time step T , indexed by $k = 0, 1, \dots$, where the time is $t = kT$. In order to account for any possible network topology, including lane-drops and lane-additions, both on the right and on the left sides of the motorway, we assume that $j = 0$ corresponds to the segment(s) including the most right lane; consequently, m_i and M_i are defined as the minimum and maximum indexes j , respectively, for which a lane exists within segment i . For example, looking at the hypothetical motorway stretch depicted in Fig. 1, $m_0 = 0$ and $M_0 = 4$, while $m_3 = 1$ and $M_3 = 3$. According to this definition, the total number of cells from the origin to segment i is $H_i = \sum_{r=0}^i (M_r - m_r + 1)$, and the total number of cells for the whole stretch is $\bar{H} = H_N$.

Each motorway cell (i, j) is characterised by the traffic density $\rho_{i,j}(k)$, defined as the number of vehicles present within the cell at time instant k divided by L_i . Density dynamically evolves according to the following conservation law equation, see e.g. [13],

$$\begin{aligned} \rho_{i,j}(k+1) = & \rho_{i,j}(k) + \frac{T}{L_i} [q_{i-1,j}(k) - q_{i,j}(k)] \\ & + \frac{T}{L_i} [f_{i,j-1}(k) - f_{i,j}(k)] + \frac{T}{L_i} d_{i,j}(k), \end{aligned} \quad (1)$$

where $q_{i,j}(k)$ is the longitudinal flow leaving cell (i, j) and entering cell $(i+1, j)$ during time interval $(k, k+1]$; $f_{i,j}(k)$ is the net lateral flow moving from cell (i, j) to cell $(i, j+1)$ during time interval $(k, k+1]$; and $d_{i,j}(k)$ is the external flow entering the network in cell (i, j) , either from the mainstream or from an on-ramp, during time interval $(k, k+1]$. Depending on the network topology, some terms of (1) may not be present. In particular, the inflow $q_{i-1,j}(k)$ does not exist for the first segment of the network, the outflow $q_{i,j}(k)$ does not exist for the last segment before a lane-drop, while lateral flow terms $f_{i,j}(k)$ exist only for $m_i \leq j < M_i$. Following previous considerations, the total number of lateral flow terms is $\bar{F} = \bar{H} - N$.

Similar modelling approaches of multi-lane motorway traffic are considered also in [13], [14], [15]. One aspect that is interesting to be pointed out is that the net lateral flow $f_{i,j}(k)$ is considered only in one direction, i.e., from right to left lanes, therefore, $f_{i,j}(k)$ is actually the difference between the flow leaving and entering lane j at its left side. This simplification is useful for the subsequent control problem formulation, since lateral flows are treated as control inputs.

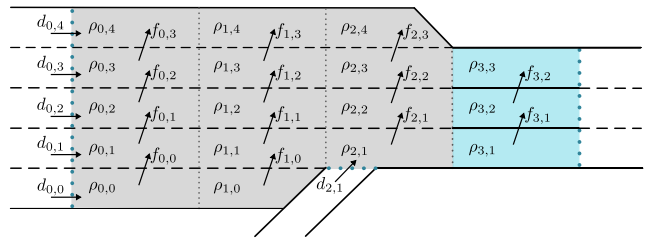


Fig. 1. A hypothetical motorway stretch.

Let us consider the well-known relation

$$q_{i,j}(k) = \rho_{i,j}(k) v_{i,j}(k); \quad (2)$$

replacing (2) into (1) we obtain

$$\begin{aligned} \rho_{i,j}(k+1) = & \frac{T}{L_i} v_{i-1,j}(k) \rho_{i-1,j}(k) + \left[1 - \frac{T}{L_i} v_{i,j}(k) \right] \rho_{i,j}(k) \\ & + \frac{T}{L_i} [f_{i,j-1}(k) - f_{i,j}(k)] + \frac{T}{L_i} d_{i,j}(k), \end{aligned} \quad (3)$$

which, treating speeds $v_{i,j}(k)$ as known parameters, can be seen as a Linear Parameter Varying (LPV) system in the form

$$\underline{x}(k+1) = A(k)\underline{x}(k) + B\underline{u}(k) + \underline{d}(k) \quad (4)$$

where (time index k is omitted to simplify notation)

$$\underline{x} = [\rho_{0,m_0} \dots \rho_{0,M_0} \ \rho_{1,m_1} \dots \rho_{N,M_N}]^T \in \mathbb{R}^{\bar{H}}, \quad (5)$$

$$\underline{u} = [f_{0,m_0} \dots f_{0,M_0} \ f_{1,m_0}(k) \dots f_{N,M_N-1}]^T \in \mathbb{R}^{\bar{F}}, \quad (6)$$

$$\underline{d} = \left[\frac{T}{L_0} d_{0,m_0} \dots \frac{T}{L_0} d_{0,M_0} \ \frac{T}{L_1} d_{1,m_1} \dots \frac{T}{L_N} d_{N,M_N} \right]^T \in \mathbb{R}^{\bar{H}}; \quad (7)$$

while $A \in \mathbb{R}^{\bar{H} \times \bar{H}}$ represents the connection between pairs of subsequent cells connected by a longitudinal flow and $B \in \mathbb{R}^{\bar{H} \times \bar{F}}$ reflects the connection of adjacent cells connected by lateral flows.

B. Optimal control problem formulation

The linear system described in Section II-A is used for formulating an optimal control problem with the purpose of manipulating the lateral flows in order to avoid the creation of congestion due to the activation of a bottleneck.

Under the assumption that the overall traffic flow entering the controlled area does not exceed the bottleneck capacity and that the controller succeeds to avoid the creation of congestion, we can assume that the speed in all cells remains at a constant value (e.g., the free flow speed) $v_{i,j}(k) \equiv \bar{v}, \forall i, j, k$, which implies that (4) can be written as a LTI system

$$\underline{x}(k+1) = A\underline{x}(k) + B\underline{u}(k) + \underline{d}. \quad (8)$$

An effective target for our control strategy is to avoid exceeding the nominal capacity of the bottleneck, which is equivalent to maintaining the density at the bottleneck area below its critical value. We define the following quadratic cost function, over an infinite time horizon, that accounts for the penalisation of the difference between some densities and pre-specified (constant) set-point values, as well as a

penalty term aiming at maintaining small control inputs, i.e., small lateral flows (weighted by φ):

$$J = \sum_{k=0}^{\infty} \left\{ \sum_{\hat{i}} \sum_{\hat{j}} \alpha_{\hat{i},\hat{j}} [\rho_{\hat{i},\hat{j}}(k) - \hat{\rho}_{\hat{i},\hat{j}}]^2 + \varphi \sum_{i=0}^N \sum_{j=m_i}^{M_i-1} [f_{i,j}(k)]^2 \right\}, \quad (9)$$

where (\hat{i}, \hat{j}) denote a targeted cell, $\hat{\rho}_{\hat{i},\hat{j}}$ is the desired set-point, and $\alpha_{\hat{i},\hat{j}}$ is the corresponding weighting parameter. We rewrite (9) in matrix form as

$$J = \sum_{k=0}^{\infty} \left\{ [C\underline{x}(k) - \underline{\hat{y}}]^T Q [C\underline{x}(k) - \underline{\hat{y}}] + \underline{u}^T(k) R \underline{u}(k) \right\}, \quad (10)$$

where $Q = Q^T \geq 0$ and $R = \varphi I_F > 0$ are weighting matrices associated to the magnitude of the state tracking error and control actions, respectively, while C reflects the cells that are tracked. At first, we may suppose to target only the cells at the bottleneck locations (i.e., in Fig. 1, $\rho_{3,1}$, $\rho_{3,2}$, $\rho_{3,3}$).

The problem (10), (8) can be solved through a Linear Quadratic Regulator (LQR), which provides a stabilising feedback control law under the assumptions that the original system is, at least, stabilisable and detectable (see Chapter 2 of [16]).

C. Stabilisability and detectability

To address stabilisability, we can see that the matrix A is, by construction, lower triangular, implying that its eigenvalues λ are equal to the elements in the main diagonal. Since \bar{v} is always positive, the modes related to segments for which another downstream segment exists are always stable ($|\lambda| < 1$), while the modes related to segments without any other segment downstream (i.e., at a lane-drop) are marginally stable ($\lambda = 1$). According to the Hautus-test [17], the system is stabilisable if, for each unstable (or marginally stable) mode, relation

$$\text{rank}[(\lambda I - A) B] = \bar{H} \quad (11)$$

is satisfied. This implies that, to guarantee that the pair (A, B) is stabilisable, B must have more linearly independent columns than the number of non-stable ($\lambda \geq 1$) modes, that is, for each lane dropping, there must be at least one controlled lane-changing, which is trivially satisfied for the defined network structure.

We turn now our attention to the detectability of the pair $(A, C^T Q C)$, which, since $Q > 0$, is equivalent to the detectability of the pair (A, C) [18]. We proceed thus with the Hautus-test [17] for the pair (A, C) , that is, if, for each unstable (or marginally stable) mode, relation

$$\text{rank} \begin{bmatrix} (\lambda I - A) \\ C \end{bmatrix} = \bar{H} \quad (12)$$

is satisfied, then the pair (A, C) is detectable. In our case, this is verified in case C has at least a non-zero element in each column corresponding to $\lambda = 1$, which implies controlling the density of each cell that does not have any other cell downstream. This requires the definition of an arbitrary set-point for the density in this cell, which is, for practical

reasons, undesirable. To account for this issue, we propose to place an additional dummy cell immediately downstream of each lane-drop, imposing it, with an appropriate high penalty weight $\alpha_{\hat{i},\hat{j}}$, to have a density equal to zero. Note that, in the described case, the system is also observable.

D. Optimal solution

The solution to the proposed LQR problem is the linear feedback/feedforward control law

$$\underline{u}^* = -K\underline{x} + \underline{u}_{\text{ff}}, \quad (13)$$

where

$$K = (R + B^T P B)^{-1} B^T P A \quad (14)$$

$$P = C^T Q C + A^T P A - A^T P B (R + B^T P B)^{-1} B^T P A \quad (15)$$

$$\underline{u}_{\text{ff}} = (R + B^T P B)^{-1} B^T F (C^T Q \underline{\hat{y}} - P \underline{d}) \quad (16)$$

$$F = (I - (A - B K)^T)^{-1}. \quad (17)$$

The feedback control law (13) is very effective for practical application since it requires the computation of the feedback gain matrix K offline. Note that the optimal gain (14) and the Algebraic Riccati Equation (15) are the same that can be found in classic Optimal Control books [19].

Note also that, the regulator (13) is a so-called state-feedback regulator, which requires availability of measurements for all state variables (densities for each cell) in real time. In the case of incomplete measurements, one may employ a traffic state estimator to produce the missing measurements, e.g., in the context of connected vehicles, [20], [21], [22].

E. Optimal set-point tuning via extremum seeking

The proposed methodology requires the knowledge of the set-points, namely the critical densities, \hat{y} for all lanes at the bottleneck location. This is, in principle, a non-trivial task that may be done by collecting traffic data (prior to the control application) and analysing the obtained fundamental diagrams, in addition to some real-time fine tuning during the controller application. On the other hand, adaptive algorithms have been proposed and employed for tuning the design parameters within urban control strategies [23], [24].

We propose here a methodology based on discrete-time extremum seeking, which is a nonmodel-based method for real-time optimisation that can be employed for tuning set-points to achieve an optimal value of a cost utilising only real-time measurements of an appropriate cost function. Extremum seeking has been widely studied and used in several applications, e.g. [12], [24], [25], [26], [27], [24]. In our case, in order to guarantee that the estimated critical densities remain within a feasible interval, we incorporate also an orthogonal projection operator (22) that prohibits the estimated parameters from leaving the interval $[\hat{y}^{\min}, \hat{y}^{\max}]$ (see, for more details, [27] and [28]).

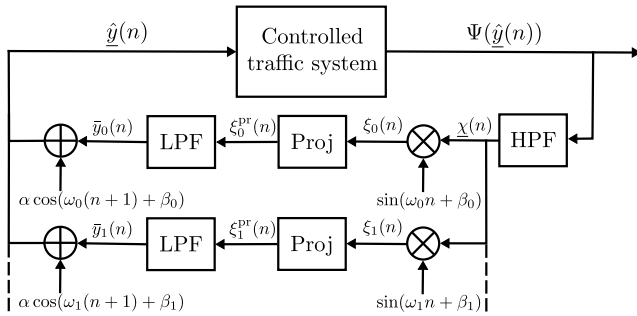


Fig. 2. The employed extremum seeking scheme.

The employed control framework for multi-parameter extremum seeking, illustrated in Fig. 2, is formulated as

$$\chi(n) = -h\chi(n-1) + \Psi(\hat{y}(n)) - \Psi(\hat{y}(n-1)) \quad (18)$$

$$\xi_\ell(n) = \chi_\ell(n) \sin(\omega_\ell n + \beta_\ell) \quad (19)$$

$$\bar{y}_\ell(n+1) = \bar{y}_\ell(n) - \text{Proj}\{\gamma \xi_\ell(n); \hat{y}^{\min}, \hat{y}^{\max}\} \quad (20)$$

$$\hat{y}_\ell(n) = \bar{y}_\ell(n) + \alpha \cos(\omega(n+1) + \beta) \quad (21)$$

where

$$\text{Proj}\{\phi; \hat{y}^{\min}, \hat{y}^{\max}\} = \begin{cases} \frac{\bar{y}_\ell - \phi - \hat{y}^{\min}}{\delta} \phi, & \text{if } \bar{y}_\ell \leq \hat{y}^{\min} + \phi + \delta \\ \frac{\hat{y}^{\max} - \bar{y}_\ell + \phi}{\delta} \phi, & \text{if } \bar{y}_\ell \geq \hat{y}^{\max} + \phi - \delta \\ \phi, & \text{otherwise.} \end{cases} \quad (22)$$

The cost function Ψ is evaluated while employing different set-points in the control strategy; $\ell = 0, \dots$ is the parameter index; n is the iteration index of the extremum seeking algorithm; \hat{y}^{\min} and \hat{y}^{\max} are physically meaningful bounds for parameters \hat{y} ; while $h, \omega_\ell, \beta_\ell, \delta, \gamma$, and α are parameters of the extremum seeking algorithm.

Since the cost function must reflect the performance of the traffic system for given set-points \hat{y} , we choose the Total Travel Time (TTT) [29] over a finite time horizon K , defined as

$$TTT = T \sum_{k=0}^K \sum_{i=0}^N L_i \sum_{j=m_i}^{M_i-1} \rho_{i,j}(k). \quad (23)$$

III. SIMULATION EXPERIMENTS

A. Nonlinear multi-lane traffic flow model

In order to test and evaluate the performance of the proposed control strategy, we present simulation experiments using a first-order traffic flow model based on [13]. The model is used for reproducing the traffic behaviour for a multi-lane motorway and it features: (i) non-linear functions for the lateral flows of manually driven vehicles; (ii) a CTM-like [30] formulation for the longitudinal flows; and (iii) a non-linear formulation to account for the capacity drop phenomenon. We provide here a brief explanation of the employed model for self-completeness.

We consider the conservation law equation (1), where all variables are defined as in Section II-A.

Lateral flows due to manual lane-changing are considered among adjacent lanes of the same segment, and corresponding rules are defined in order to properly assign and bound

their values. Lateral flows are computed as

$$f_{i,j}(k) = l_{i,j,j+1}(k) - l_{i,j+1,j}(k), \quad (24)$$

where

$$l_{i,\bar{j},j}(k) = \min \left\{ 1, \frac{S_{i,j}(k)}{D_{i,j-1,j}(k) + D_{i,j+1,j}(k)} \right\} D_{i,\bar{j},j}(k) \quad (25)$$

$$S_{i,j}(k) = \frac{L_i}{T} [\rho_{i,j}^{\text{jam}} - \rho_{i,j}(k)] \quad (26)$$

$$D_{i,j}(k) = \frac{L_i}{T} \rho_{i,j}(k) A_{i,j,\bar{j}}(k) \quad (27)$$

$$A_{i,j,\bar{j}}(k) = \mu \max \left\{ 0, \frac{G_{i,j,\bar{j}}(k) \rho_{i,j}(k) - \rho_{i,\bar{j}}(k)}{G_{i,j,\bar{j}}(k) \rho_{i,j}(k) + \rho_{i,\bar{j}}(k)} \right\}, \quad (28)$$

and $\bar{j} = j \pm 1$. S denotes the available space, in terms of flow acceptance, while D denotes the lateral demand flow, which is computed via definition of the attractiveness rate A .

Longitudinal flows are the flows going from a segment to the next downstream one, while remaining in the same lane. We employ the Godunov-discretised first-order model proposed in [13], employing however a non-linear exponential demand function for under-critical densities, as proposed in [31], to obtain a more realistic behaviour at low densities. The model accounts also for the capacity drop phenomenon via a linearly decreasing demand function for over-critical densities. Also, a linear reduction of the maximum flow as a function of the entering lane-changing flows is included, to account for the nuisance caused by lane changing manoeuvres. More details and calibration results related to this model are presented in [13].

The overall formulation for longitudinal flow is

$$q_{i,j}(k) = \min \{ Q_{i,j}^D(k), Q_{i+1,j}^S(k) - d_{i,j}(k) \}, \quad (29)$$

where

$$Q_{i,j}^D(k) = \begin{cases} v_{i,j}^{\max} \exp \left[-\frac{1}{\alpha} \left(\frac{\rho_{i,j}(k)}{\rho_{i,j}^{\text{cr}}} \right)^\alpha \right] \rho_{i,j}(k), & \text{if } \rho_{i,j}(k) < \rho_{i,j}^{\text{cr}} \\ \frac{(1-\gamma) Q_{i,j}^{\text{cap}}}{\rho_{i,j}^{\text{cr}} - \rho_{i,j}^{\text{jam}}} [\rho_{i,j}(k) - \rho_{i,j}^{\text{jam}}] + Q_{i,j}^B(k), & \text{otherwise} \end{cases} \quad (30)$$

$$Q_{i+1,j}^S(k) = \begin{cases} Q_{i+1,j}^{\text{cap}}, & \text{if } \rho_{i+1,j}(k) < \rho_{i+1,j}^{\text{cr}} \\ w_{i+1} [\rho_{i+1,j}^{\text{jam}} - \rho_{i+1,j}(k)], & \text{otherwise.} \end{cases} \quad (31)$$

$$Q_{i,j}^B(k) = \gamma Q_{i,j}^{\text{cap}} - \eta [l_{i,j+1,j}(k) + l_{i,j-1,j}(k)] \quad (32)$$

Parameter v^{\max} denotes the maximum speed, Q^{cap} is the capacity flow, ρ^{cr} is the critical density (i.e., the density at which the capacity flow occurs), while $\alpha = \left(\ln \frac{Q^{\text{cap}}}{v^{\max} \rho^{\text{cr}}} \right)^{-1}$ [31]. Parameter γ influences the impact of capacity drop due to overcritical densities, while η affects the impact of entering lane-changing flows on the segment capacity.

B. Network description and the no-control case

We consider a hypothetical motorway stretch to test and evaluate the performance of the proposed strategy. In particular, we consider the network depicted in Fig. 3, which is composed of 7 segments; segments 1, ..., 5 feature three lanes, while segments 6 and 7 feature only two lanes, with a lane-drop located downstream of cell (5, 1). All segments

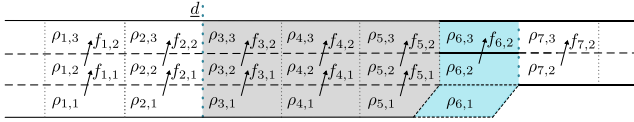


Fig. 3. The motorway stretch used for testing and evaluating the proposed control strategy.

TABLE I
PARAMETERS USED IN THE NONLINEAR MULTI-LANE TRAFFIC FLOW MODEL

	Scenario 1		Scenario 2	
	$j = 1, 2$	$j = 3$	$j = 1, 2$	$j = 3$
v^{\max} [km/h]	100	120	100	120
Q^{cap} [veh/h]	1800	2400	1800	2400
ρ^{cr} [veh/km]	32	36	32	36
ρ^{jam} [veh/km]	120	160	120	160
γ	0.6	0.6	0.6	0.6
η	0	0	0.06	0.06
G	1	1	1	1
μ	0.6	0.6	0.6	0.6

are characterised by the same length $L_i = 0.5$ km, while we define a simulation step $T = 10$ s. Different lanes feature different parameters, namely a different FD, which may reflect different traffic composition (e.g., a high number of heavy vehicles reducing the capacity of a specific lane). Two scenarios are defined: in Scenario 1, capacity drop is assumed to be caused only by over-critical densities (i.e., $\eta = 0$), while in Scenario 2, the complete capacity drop formulation is used. The employed parameters are shown in Table I.

Traffic demand profiles are defined for a simulation horizon $K = 80$ min, generated perturbing trapezoidal-like shapes with additive zero-mean Gaussian white noise and the overall demand entering the network is, at its peak, roughly equivalent to the total capacity of segment 5 (where the lane-drop occurs).

Running the macroscopic model (1), (24)–(32) without the use of any control actions for Scenario 1 produces a strong traffic congestion starting at the lane-drop area, due to non-optimal spontaneous lane-assignment of vehicles. Inspecting the contour plots shown in Fig. 4, we can see that the density increases firstly in lane 1 (the one that is dropping) at around $t = 10$ min due to the high demand arriving in the lane-drop area, while vehicles try to merge first into lane 2, and, due to the fact that density increases also in this lane, eventually also into lane 3. In particular, most lane-changes take place within segment 5 (see Fig. 5 (top)), while their intensity progressively reduces upstream, with almost no lane-changes in segment 1. Note that, according to (28) and with $G_{i,j,\bar{j}} = 1$, the lane-changing model acts towards the homogenisation of the densities between adjacent lanes. The detrimental effects of the congestion worsen as a consequence of the occurring capacity drop, which is here triggered by overcritical densities at all lanes of segment 5, causing a reduction of the outflow in both lanes, as shown

in Fig. 6 (top).

The created congestion spills back covering several segments upstream in all lanes, in particular reaching segment 2 (see Fig. 4). As numerical evaluation criterion we employ the TTT, obtaining, for the no-control case of Scenario 1, a resulting overall TTT = 306.1 veh · h.

For Scenario 2, the congestion pattern is basically similar, however with a more extended congestion both in time and space (reaching segment 1), due to the capacity reduction resulting from lane changes, with a corresponding TTT = 377.4 veh · h.

C. Application of the proposed control strategy

We proceed now to the evaluation of the proposed control strategy in the scenario described in Section III-B. We define as “application area”, namely the portion of network where we apply our designed strategy, the area from segment 3 to segment 6 (see Fig. 3). We use the outflow of the segments immediately upstream of the application area $q_{2,j}$ as our demand \underline{d} . A dummy cell (6, 1) is added immediately downstream of the lane-drop, as proposed in Section II-C. The set-point considered in the LQR includes therefore all cells in segment 6.

According to the network topology and setting a constant speed $\bar{v} = 100$ km/h and cost weights $Q_{i,j} = 1$, for $i = j = 2, 3$; $Q_{i,j} = 100$, for $i = j = 1$; $Q_{i,j} = 0$; $\forall i \neq j$; $\varphi = 10^{-5}$ (obtained after some manual tuning of the controller aiming at achieving an efficient and smooth response), we compute (offline) the gains as described in Section II-D.

We assume to know the critical densities at the controlled area which are used to build the set-point vector \hat{y} , namely $\hat{\rho}_{6,2} = 32$ veh/km, $\hat{\rho}_{6,3} = 36$ veh/km, while at the additional dummy segment we define $\hat{\rho}_{6,1} = 0$ veh/km.

Lateral flows $f_{i,j}$ are computed as \underline{u}^* , via the optimal control law (13), and are then applied directly in the conservation law equation (1), while longitudinal flows $q_{i,j}$ are obtained from (29)–(31) as in the no-control case.

From inspection of the resulting contour plots in Fig. 7, we can see that the controller is capable of avoiding congestion. This is due to the fact that, during the period characterised by a high demand, the density at the bottleneck area is maintained at its critical value. The optimal lateral flows are distributed quite homogeneously within the whole application area (see Fig. 5 (bottom)), thus avoiding high lane-changing flows close to the lane-drop location. Moreover, since all densities remain undercritical, the capacity drop phenomenon is not appearing and the system is operating around the bottleneck capacity during the whole peak period (see Fig. 6 (bottom)). Within this scenario, we obtain a TTT = 188.3 veh · h, which is a 38.5% improvement with respect to the no-control case.

The proposed control strategy applied to Scenario 2 produces the same traffic behaviour as Scenario 1, where TTT = 188.3 veh · h, which, in this case, corresponds to a 50.1% improvement with respect to the no-control case.

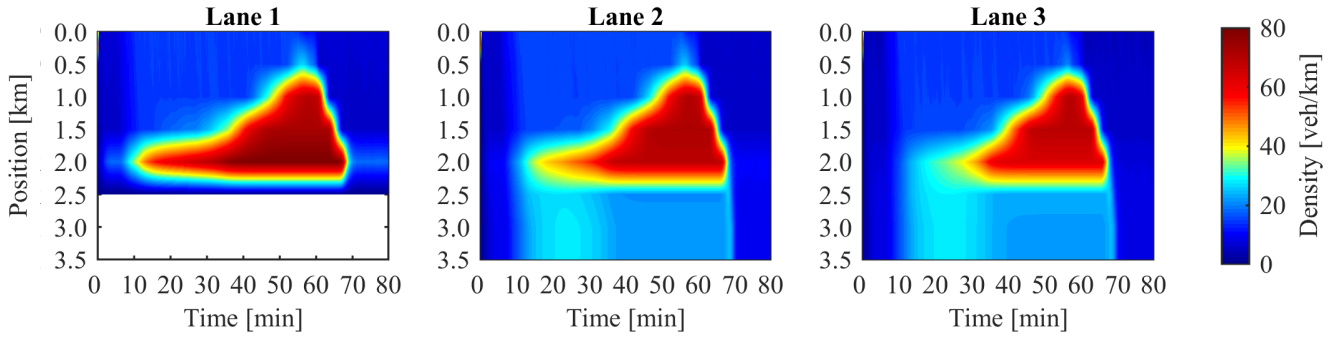


Fig. 4. Contour plots of densities in the no-control case for Scenario 1.

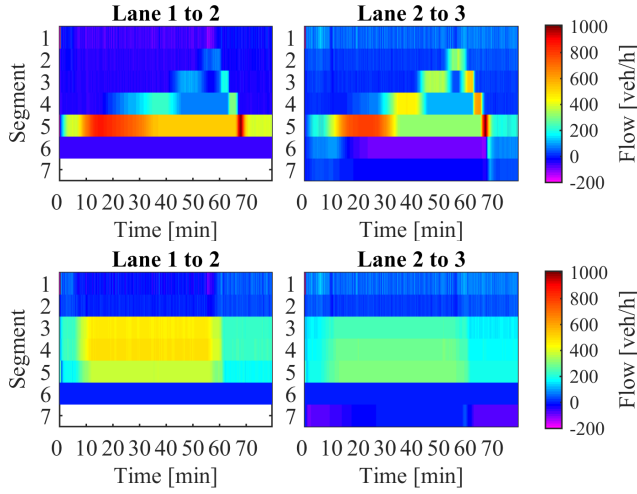


Fig. 5. Contour plots of net lateral flows in the no-control case (top) and in case control is applied to Scenario 1 (bottom).

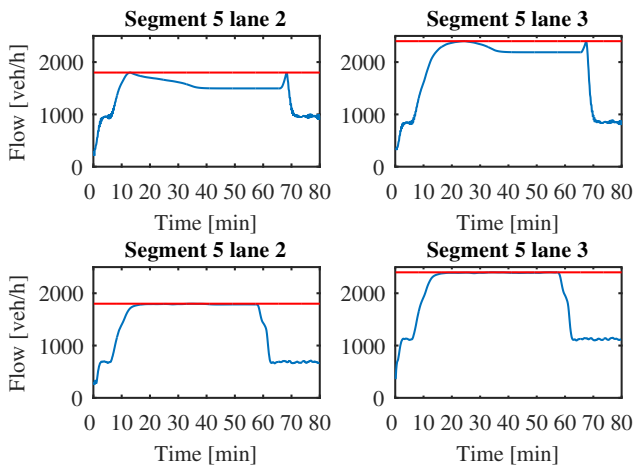


Fig. 6. The flow exiting from lanes 2 (left) and 3 (right) of segment 5 (blue lines) and the corresponding capacity flow (red lines). In the no-control case (top), the capacity drop mechanism is triggered and the outflow cannot reach the capacity flow. Whereas, when control is applied to Scenario 1 (bottom), the capacity drop phenomenon is avoided, even during the peak period, and the outflow is close to the bottleneck capacity.

TABLE II
PARAMETERS OF THE EXTREMUM SEEKING ALGORITHM

h	0.9	\hat{y}^{\min} [veh/km]	28
ω_n [rad]	$\frac{\pi}{1.5}$	\hat{y}^{\max} [veh/km]	42
β_1 [rad]	0	γ	0.05
β_2 [rad]	$\frac{\pi}{2}$	α	0.5
δ [veh/km]	2		

D. Optimal set-point seeking

The results presented in Section III-C are based on the knowledge of the exact value of critical densities at the bottleneck location. To overcome a situation where these values may be unknown, we test here the effectiveness of the algorithm for finding the optimal set-points proposed in Section II-E. We employ Scenario 1 of Section III-C, computing the TTT for the controlled area (from segment 3 to segment 6) over a horizon $K = 80$ min, which corresponds to one iteration of the extremum seeking algorithm, and using the cost $\Psi = -\text{TTT}$. This procedure is iteratively performed for S times, in our case with $S = 400$. The set of parameters used in the algorithm is presented in Table II.

The critical densities are initialised as $\hat{\rho}_{6,2} = 38$ veh/km, $\hat{\rho}_{6,3} = 30$ veh/km, which represents a non-optimal set-point configuration for the LQR controller. As shown in Fig. 8, the proposed algorithm achieves the optimal cost, while also reaching and maintaining the optimal density set-points.

IV. CONCLUSIONS

We proposed and tested an optimal adaptive control strategy for lane-changing-based traffic control at bottleneck locations, assuming that vehicles are equipped with VACS, capable of receiving and executing lane-changing commands.

Future work includes the extension of this methodology to account for unmeasured demand flows and incomplete measurements. Moreover, we are looking into the case of mixed traffic, where manual vehicles may not follow the prescribed lane-changing commands; as well as into testing the methodology on a microscopic simulation environment.

REFERENCES

- [1] C. Diakaki, M. Papageorgiou, I. Papamichail, and I. K. Nikolos, "Overview and analysis of vehicle automation and communication

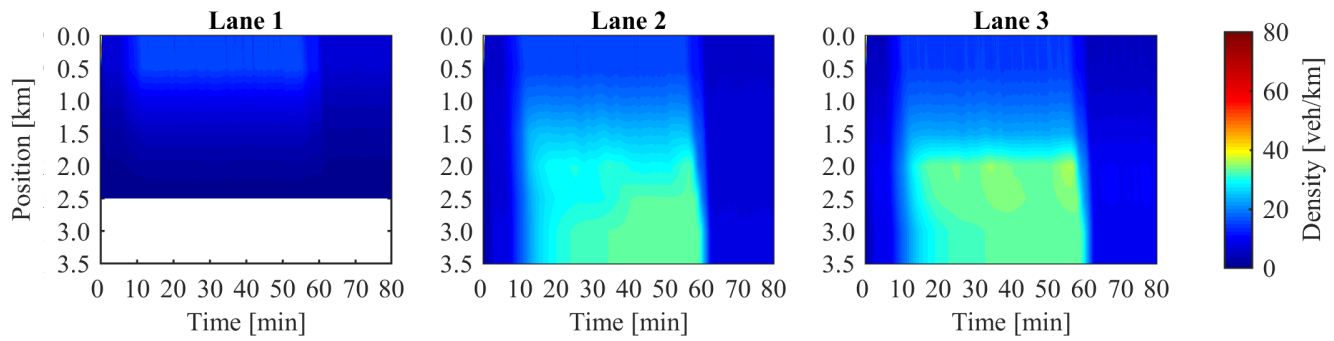


Fig. 7. Contour plots of densities when the proposed control strategy is applied to Scenario 1.

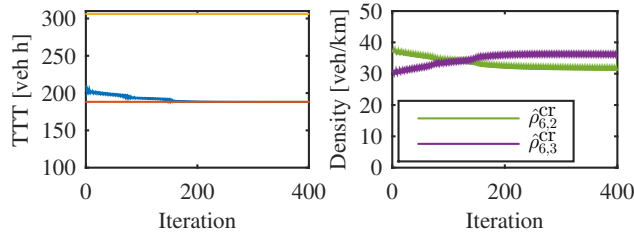


Fig. 8. The cost function (left) in the no-control case (yellow), optimum achieved setting critical densities as set-points (red), and applying the extremum seeking algorithm (blue); and the optimal set-points achieved by the extremum seeking algorithm (right).

systems from a motorway traffic management perspective,” *Transportation Research Part A: Policy and Practice*, vol. 75, pp. 147 – 165, 2015.

- [2] M. Cassidy and R. Bertini, “Observations at a freeway bottleneck,” in *Proceedings of the 14th International Symposium on Transportation and Traffic Theory*, 1999, pp. 107–124.
- [3] Y. Zhang and P. A. Ioannou, “Combined variable speed limit and lane change control for truck-dominant highway segment,” in *IEEE 18th International Conference on Intelligent Transportation Systems (ITSC)*, 2015, pp. 1163–1168.
- [4] P. Varaiya, “Smart cars on smart roads: problems of control,” *IEEE Transactions on Automatic Control*, vol. 38, no. 2, pp. 195–207, 1993.
- [5] B. Rao and P. Varaiya, “Roadside intelligence for flow control in an intelligent vehicle and highway system,” *Transportation Research Part C: Emerging Technologies*, vol. 2, no. 1, pp. 49–72, 1994.
- [6] P. Y. Li, R. Horowitz, L. Alvarez, J. Frankel, and A. M. Robertson, “An Automated Highway System link layer controller for traffic flow stabilization,” *Transportation Research Part C: Emerging Technologies*, vol. 5, no. 1, pp. 11–37, 1997.
- [7] K. Kim, J. V. Medanić, and D. I. Cho, “Lane assignment problem using a genetic algorithm in the Automated Highway Systems,” *International Journal of Automotive Technology*, vol. 9, no. 3, pp. 353–364, 2008.
- [8] L. D. Baskar, B. De Schutter, and H. Hellendoorn, “Traffic management for automated highway systems using model-based predictive control,” *IEEE Transactions Intelligent Transportation Systems*, vol. 13, no. 2, pp. 838–847, 2012.
- [9] C. Roncoli, I. Papamichail, and M. Papageorgiou, “Hierarchical model predictive control for multi-lane motorways in presence of Vehicle Automation and Communication Systems,” *Transportation Research Part C: Emerging Technologies*, vol. 62, pp. 117–132, 2016.
- [10] C. Roncoli, M. Papageorgiou, and I. Papamichail, “Traffic flow optimisation in presence of Vehicle Automation and Communication Systems - Part II: Optimal control for multi-lane motorways,” *Transportation Research Part C*, vol. 57, pp. 260 – 275, 2015.
- [11] M. Guériau, R. Billot, N.-E. E. Faouzi, S. Hassas, and F. Armetta, “X2V-based information dissemination for highway congestion reduction,” in *18th Euro Working Group on Transportation (EWGT)*, Delft, the Netherlands, 2015.
- [12] K. B. Ariyur and M. Krstić, *Real-time optimization by extremum-seeking control*. John Wiley & Sons, Inc., 2003.
- [13] C. Roncoli, M. Papageorgiou, and I. Papamichail, “Traffic flow optimisation in presence of Vehicle Automation and Communication Systems - Part I: A first-order multi-lane model for motorway traffic,” *Transportation Research Part C*, vol. 57, pp. 241 – 259, 2015.
- [14] P. Munjal and L. Pipes, “Propagation of on-ramp density perturbations on unidirectional two- and three-lane freeways,” *Transportation Research*, vol. 5, no. 4, pp. 241–255, 1971.
- [15] P. G. Michalopoulos, D. E. Beskos, and Y. Yamauchi, “Multilane traffic flow dynamics: Some macroscopic considerations,” *Transportation Research Part B: Methodological*, vol. 18, no. 4-5, pp. 377–395, 1984.
- [16] F. L. Lewis, D. L. Vrabie, and V. L. Szymos, *Optimal Control*. John Wiley & Sons, Inc., 2012.
- [17] R. L. Williams and D. A. Lawrence, *Linear state-space control systems*. Hoboken, NJ, USA: John Wiley & Sons, Inc., 2007.
- [18] J. P. Hespanha, *Linear Systems Theory*. Princeton Press, 2009.
- [19] B. D. O. Anderson and J. B. Moore, *Linear optimal control*. Prentice-Hall, 1971.
- [20] N. Bekiaris-Liberis, C. Roncoli, and M. Papageorgiou, “Highway traffic state estimation with mixed connected and conventional vehicles,” *IEEE Transactions Intelligent Transportation Systems*, to appear.
- [21] T. Seo, T. Kusakabe, and Y. Asakura, “Estimation of flow and density using probe vehicles with spacing measurement equipment,” *Transportation Research Part C: Emerging Technologies*, vol. 53, pp. 134–150, 2015.
- [22] J. C. Herrera and A. M. Bayen, “Incorporation of lagrangian measurements in freeway traffic state estimation,” *Transportation Research Part B: Methodological*, vol. 44, no. 4, pp. 460–481, 2010.
- [23] A. Kouvelas, K. Aboudolas, E. B. Kosmatopoulos, and M. Papageorgiou, “Adaptive performance optimization for large-scale traffic control systems,” *IEEE Transactions on Intelligent Transportation Systems*, vol. 12, no. 4, pp. 1434–1445, 2011.
- [24] R. Kutadinata, W. Moase, C. Manzie, L. Zhang, and T. Garoni, “Enhancing the performance of existing urban traffic light control through extremum-seeking,” *Transportation Research Part C: Emerging Technologies*, vol. 62, pp. 1 – 20, 2016.
- [25] Joon-Young Choi, M. Krstic, K. Ariyur, and J. Lee, “Extremum seeking control for discrete-time systems,” *IEEE Transactions on Automatic Control*, vol. 47, no. 2, pp. 318–323, 2002.
- [26] N. Killingsworth and M. Krstic, “PID tuning using extremum seeking: online, model-free performance optimization,” *IEEE Control Systems Magazine*, vol. 26, no. 1, pp. 70–79, 2006.
- [27] P. Frihauf, M. Krstic, and T. Baar, “Finite-horizon LQ control for unknown discrete-time linear systems via extremum seeking,” *European Journal of Control*, vol. 19, no. 5, pp. 399 – 407, 2013.
- [28] G. Mills and M. Krstic, “Constrained extremum seeking in 1 dimension,” in *53rd IEEE Conference on Decision and Control*, Los Angeles, CA, USA, 2014, pp. 2654–2659.
- [29] M. Papageorgiou, H. Hadj-Salem, and J.-M. Blossville, “ALINEA: a local feedback control law for on-ramp metering,” *Transportation Research Record*, vol. 1320, pp. 58–64, 1991.
- [30] C. F. Daganzo, “The cell transmission model: A dynamic representation of highway traffic consistent with the hydrodynamic theory,” *Transportation Research Part B: Methodological*, vol. 28, no. 4, pp. 269–287, 1994.
- [31] A. Messmer and M. Papageorgiou, “METANET: A macroscopic simulation program for motorway networks,” *Traffic Engineering & Control*, vol. 31, no. 9, pp. 466–470, 1990.